

Use of Parabolic Trough Collector as Direct Vapor Generator for an Absorption Machine: Experimental Study

Antonio Famiglietti¹, Berat Celik¹, Antonio Lecuona-Neumann¹, Ricardo López¹, José Nogueira-Goriba¹

¹ Grupo ITEA. Departamento de Ingeniería Térmica y de Fluidos, Universidad Carlos III de Madrid, Avda. de la Universidad 30, 28911 Leganés, Madrid, (Spain)

Abstract

Parabolic concentrating solar collectors PTCs represent an alternative to fossil fuel as a medium temperature heat source for a variety of applications, either in medium and small scale facilities. This work presents an innovative solution using PTCs for driving an absorption machine AM. In the novel layout proposed, the working pair of the AM circulates into the solar receiver tube, allowing refrigerant evaporation without the need of a heat transfer fluid HTF, neither a heat exchanger HX. An experimental installation has been developed and tested using Ammonia/Lithium Nitrate as the AM working pair. The preliminary results reported confirm the feasibility of the direct refrigerant vapor generation inside a PTC, encouraging further investigation to lower complexity and cost.

Parabolic Trough Collector, Absorption Machine, Ammonia/Lithium Nitrate, Solar Heating and Cooling

1. Introduction

Absorption machines (AMs) are receiving growing attention for solar heating and cooling applications (Mauthner & Weiss, 2013) due to their capability of producing heat or cold while consuming medium temperature heat instead of mechanical power (consumed as electricity), as done by a conventional inverse Rankine cycle heat pump. In fact, a thermochemical compressor replaces the mechanical vapor compressor (Herold, Radermacher, & Klein., 2016): the refrigerant vapor coming from the evaporator is absorbed at low pressure by a liquid solution, then it is pumped to the desorber/generator where the refrigerant is again separated from the solution, consuming heat from an external source. The refrigerant vapor generated goes to the condenser to close the cycle.

Heat to drive the generator can be provided by a variety of sources including natural gas combustion, waste heat from upstream thermal processes, or solar thermal energy. Various systems have been investigated to supply solar thermal energy to an AM, such as flat plate collectors FPCs and evacuated tube collectors ETCs, which allow relatively low driving temperatures, typically below 100 °C, thus limiting the *COP* of the AM. Higher *COP* can be reached using a double effect AM (Ventas, Lecuona, Vereda, & Rodriguez-Hidalgo, 2017) which requires a higher driving temperature at the generator (100 °C to 250 °C). For this purpose concentrating solar collectors can be used, either of the linear Fresnel or the Parabolic trough type since they are able to provide medium temperature heat. More information on solar driven absorption machines and advanced cycles can be found in (Wu, Wang, Shi, & Li, 2014). The availability of small and medium-scale commercial concentrating collectors encourage this possibility, also considering that their unitary price (cost per watt peak) has reached a level that is comparable to flat plate and evacuated tube collectors (~250 €/W_p), thanks to concentrated solar power technology development (National Renewable Energy Laboratories (NREL), 2015).

In a solar-driven AM facility, a heat transfer fluid HTF is typically used to receive and carry solar heat to the AM vapor generator, which is transferred to the evaporating dissolution through a heat exchanger HX (Best & Rivera, 2015). This layout increases the complexity and the costs of the overall installation besides to introduce several critical issues as HTF thermal degradation, risk of leakages, and corrosion, which complicates the competition with the attractive PV-HP technology.

(Lecuona, Famiglietti, & Legrand, 2019) proposed a simpler layout to the one described above. In order to reduce complexity and cost, the HTF and the HX are eliminated by directly evaporating the working AM dissolution inside the receiver tube of the solar collector, see Fig.1, as described in the following section. They also provide wide information on solar driven absorption solutions.

This paper describes the layout and offers information on its performances. For the layout description and

information on the flow phenomena, Section 2 is provided. It prepares to understand the results of an experimental campaign on a prototype, which has been previously numerically modeled.

2. Direct vapor generation

Fig. 1 shows the proposed concept of a direct vapor generation using a PTC collector for driving a single effect air-cooled absorption machine.

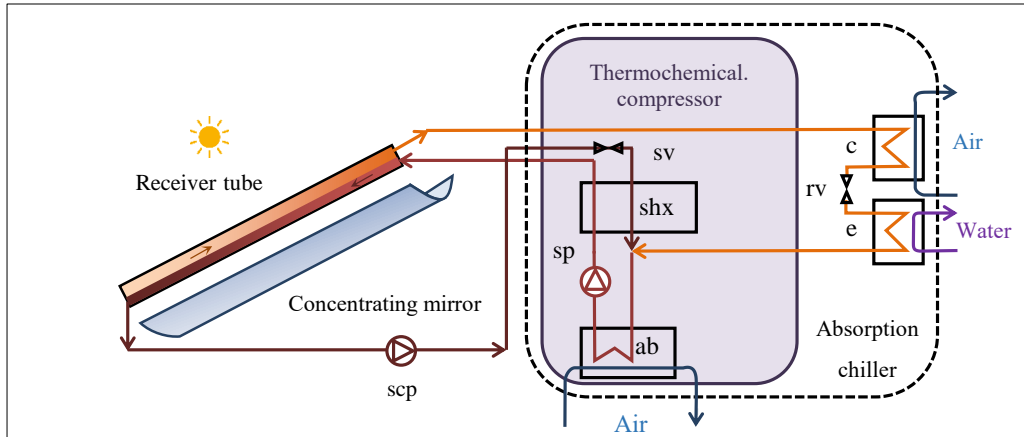


Fig. 1 Proposed layout of single effect absorption machine (AM) using a PTC as a vapor generator.

The liquid solution, rich in refrigerant, is fed to the receiver tube, which holds some degree of tilt over the horizontal line. Liquid flow does not fill the overall cross-section but only the bottom of the tube, flowing driven by gravity, at free-falling speed $\sim 1 \text{ m s}^{-1}$. The liquid solution is heated along the tube length so that refrigerant evaporates under saturation conditions at constant pressure. This vapor fills the upper part of the tube cross-section. The tube lower outlet is closed for the vapor flow so that the produced refrigerant goes upward exiting the receiver tube from its upper end. A stratified two-phase countercurrent flow takes place inside the tube, separating liquid from vapor by gravity. Although the concept is extensible to several working fluids, it has been applied to Ammonia-Lithium Nitrate solution. This is in order to benefit from the advantages of the excellent properties of ammonia as refrigerant, at the same time eliminating the drawbacks of the expensive rectification tower needed with ammonia/water solution. Freezing problems and corrosion issues are also much reduced, which are typically found with the much-used Ammonia-Water dissolution (Ventas, Lecuona, Vereda, & Rodriguez-Hidalgo, 2017).

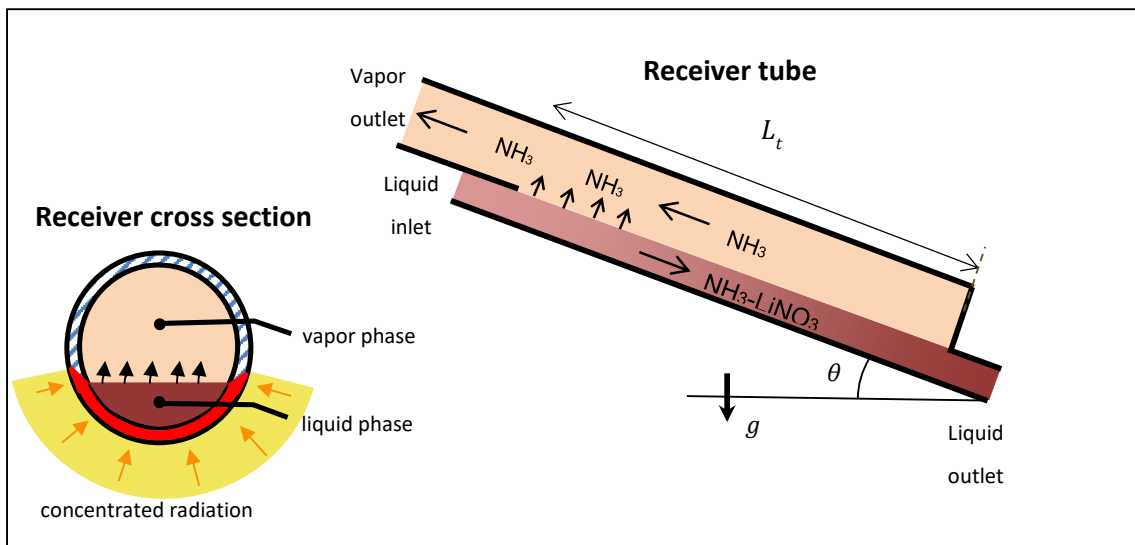


Fig. 2 Stratified two-phase flow, driven and separated by gravity, inside the solar receiver tube.

(Lecuona, Famiglietti, & Legrand, 2019) offers a detailed numerical model of the stratified two-phase flow inside the receiver tube. They developed a steady-state one-dimensional discretized mathematical model, including vapor ammonia and Ammonia/Lithium Nitrate solution properties in order to investigate the direct generator performances.

As indicated in Fig. 2, the incoming solar flux is supposed to be transferred to the liquid phase, due to much higher wall-to-liquid heat transfer compared with wall-to-gas heat transfer. The ammonia/lithium nitrate solution is fed to the receiver tube at a specific inlet temperature $T_{l,in}$ close to the saturation temperature $T_s(x_{in}, p_{in})$, although in general terms it can hold some degree of subcooling $\Delta T_{sub,in} = T_s(x_{in}, p_{in}) - T_{l,in}$. Saturation temperature depends on the working pressure p_{in} as well as ammonia mass fraction in the liquid dissolution x_{in} . Either p_{in} than x_{in} depend on the AM working conditions. For $\Delta T_{sub,in} > 0$ a subcooled region establish for a certain length downstream the receiver entrance, where the solution is heated without any ammonia evaporation until the saturation temperature is reached. Here, the incoming heat flux goes to the solution as sensible heat. In reality, subcooled boiling takes place a few degrees below the saturation temperature when the wall temperature locally exceeds the saturation temperature (Hsu, 1962). Besides increasing the heat transfer coefficient, as a consequence of bubbles formation and collapse at the surface, subcooled boiling can produce moderate subcooled refrigerant evaporation, when bubbles are large enough to reach the vapor-liquid interphase (Dorra, Lee, & Bankoff, 1993). Once the solution saturation temperature is reached, a saturated region begins. Ammonia boiling and evaporation is intense, driven by the solar heat flux. Ammonia mass fraction in the solution decreases along the tube length as consequence of evaporation. At constant pressure, under the hypothesis of saturation condition, this corresponds to an increase in solution saturation temperature, $T_l = T_s(x, p)$. As common in falling film evaporation, during saturated evaporation the incoming heat flux is then split into two component, one goes as latent heat to evaporate ammonia from the solution, while the second goes as sensible heat, increasing the liquid flow temperature up to $T_l = T_s(x, p)$. (Lecuona, Famiglietti, & Legrand, 2019) discuss this issue in details. They simulated the liquid flow evolution along the tube length L_t including the subcooled region. Fig. 3 shows the liquid temperature T_l and T_s for $p = 13.5$ bar and $x_{in} = 0.49$. The receiver tube wall temperature T_w is assumed uniform at each tube cross-section, for a given tube local thermal efficiency. Coherently with the expected operating conditions, the liquid solution is supposed to enter the generator with a few degrees of subcooling, set to $\Delta T_{sub,in} = 15$ K for the reference case.

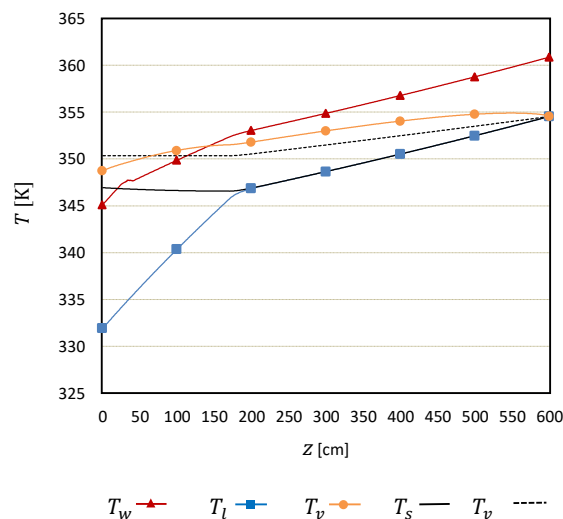


Fig. 3 Temperature of a numerical simulation considering a 6 m long parabolic trough collector with an aperture width $L_a = 2.3$ m, an optical efficiency $\eta_o = 0.71$ and a tilt angle on the horizontal $\theta = 25^\circ$, standard conditions for ambient air and irradiation over the collector surface of $G_{bT} = 800 \text{ W m}^{-2}$. Inlet liquid mass flow rate $\dot{m}_{l,in} = 0.05 \text{ kg s}^{-1}$

Fig.4 reveals the variation of ammonia mass fraction x along the axial coordinate z as a consequence of evaporation, while x_s corresponds to saturation mass fraction at the solution temperature T_l . As introduced above, a vapor flow arises from the low tube entrance up to the liquid entrance, countercurrent to liquid flow, occupying the upper part of the tube cross-section as in Fig. 2. In Fig. 4 the resulting vapor mass flow rate increases from zero at the lower end up to $\dot{m}_{v,out}$. Vapor temperature T_v is reported in Fig. 3.

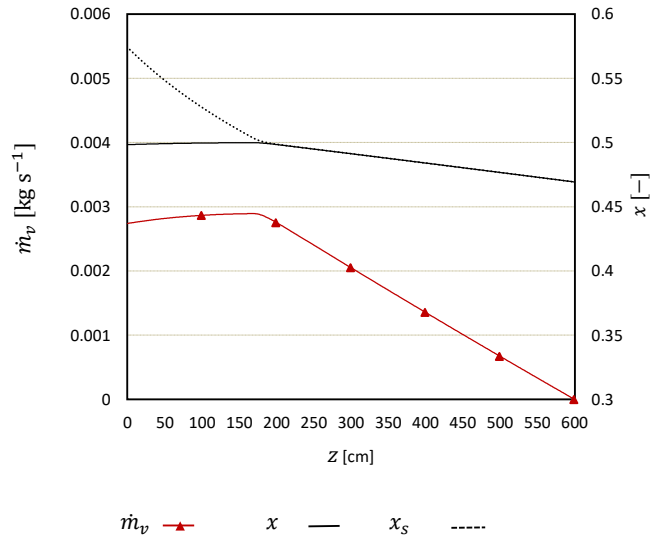


Fig. 4. Ammonia mass fraction and mass flow rate simulation considering a 6 m long parabolic trough collector with an aperture width $L_a = 2.3$ m, an optical efficiency $\eta_o = 0.71$ and a tilt angle on the horizontal $\theta = 25^\circ$, standard conditions for ambient air and irradiation over the collector surface of $G_{bT} = 800 \text{ W m}^{-2}$. Inlet liquid mass flow rate $\dot{m}_{l,in} = 0.05 \text{ kg s}^{-1}$

Heat flux partitioning between latent heat contribution to ammonia evaporation q_{ev} and sensible solution heating q_l has been numerically simulated by (Lecuona, Famiglietti, & Legrand, 2019) as reported in Fig. 5. The overall thermal power delivered to liquid $Q_w = \int_0^{L_t} q_w(z) dz$ is represented by the area below the incoming heat flux curve $q_w = q_{ev} + q_l$.

The thermal power that produces ammonia evaporation is $Q_{ev} = \int_0^{L_t} q_{ev}(z) dz$. It corresponds to the area below the q_{ev} curve, while $Q_l = Q_w - Q_{ev}$ is responsible for dissolution heating. The variation of wall-to-liquid heat transfer coefficient h_{eq} from the non-boiling entrance region to subcooled and saturated boiling regions can be observed on the second axis in Fig. 5.

Further theoretical simulation of the direct solar generator performances considering a variety of air-cooled single-stage AM working conditions can be found in (Famiglietti, Lecuona-Neumann, Nogueira, & Celik, 2018).

The following paragraphs offer an experimental study of the proposed layout.

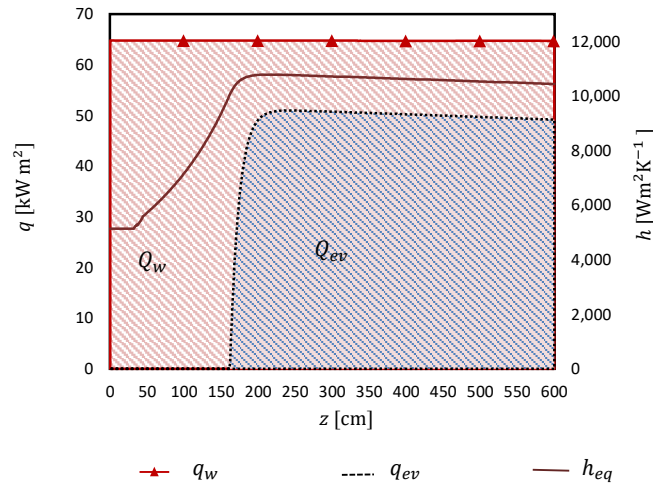


Fig. 5. Heat flux partitioning simulation considering a 6 m long parabolic trough collector with an aperture width $L_a = 2.3$ m, an optical efficiency $\eta_o = 0.71$ and a tilt angle on the horizontal $\theta = 25^\circ$, standard conditions for ambient air and irradiation over the collector surface of $G_{br} = 800 \text{ W m}^{-2}$. Inlet liquid mass flow rate $\dot{m}_{l,in} = 0.05 \text{ kg s}^{-1}$

3. Experimental setup

A prototype has been designed and installed at the Carlos III University of Madrid. A commercial parabolic trough collector (SMIRRO™) is used as a direct generator, having an aperture width $L_a = 1.3$ m and a length $L_t = 3$ m. The manufacturer gives an optical efficiency of $\eta_0 = 0.7$. The receiver tube has the same length L_t , and an internal diameter $D = 30$ mm, with 2 mm stainless steel wall thickness. A low emissivity selective coating covers the external tube surface. A glass tube, coaxial to the receiver, limits thermal losses to ambient although no vacuum condition is kept in the gap, which is filled by air at atmospheric pressure. The collector is oriented N-S and it is equipped with a single-axis sun tracking system. In order to investigate the effect of collector tilt angle on the generator performances, a dedicated elevation system allows adjusting the tilt angle between 0° and 45° .

Fig.6 displays the experimental layout. The complete AM layout shown in Fig. 1 has been simplified, excluding the evaporator and the condenser; thus, only the thermochemical compressor has been implemented. The present setup enables to test the direct solar generator approaching identical operating conditions as in a full single-effect AM. The solution pump is equipped with a frequency converter enabling to regulate the mass flow rate \dot{m}_{lin} and the pressure p_{in} at the receiver tube inlet. An electrical heater is used to adjust the solution inlet temperature T_{lin} . A separator tank is installed at the receiver tube outlet in order to evacuate residual vapor ammonia bubbles from the liquid solution and to avoid tube flooding. Being the separator partially filled by liquid solution, ammonia vapor can be evacuated only from the upper end. The evaporated ammonia mass flow rate \dot{m}_v goes to the absorber through an automatic refrigerant valve, which contributes to regulate the pressure level in the generator, together with the automatic solution valve. Three Coriolis-type Micromotion® flowmeters are used to measure mass flow rate, density, and temperature. Inlet ammonia mass fraction in the liquid solution x_{in} is calculated from density measurement using proper correlations (Libotean, Salavera, Valles, Esteve, & Coronas, 2007). Pressure and temperature are measured in several reference points of the circuit. Global and diffuse solar irradiance are measured using two pyranometers.

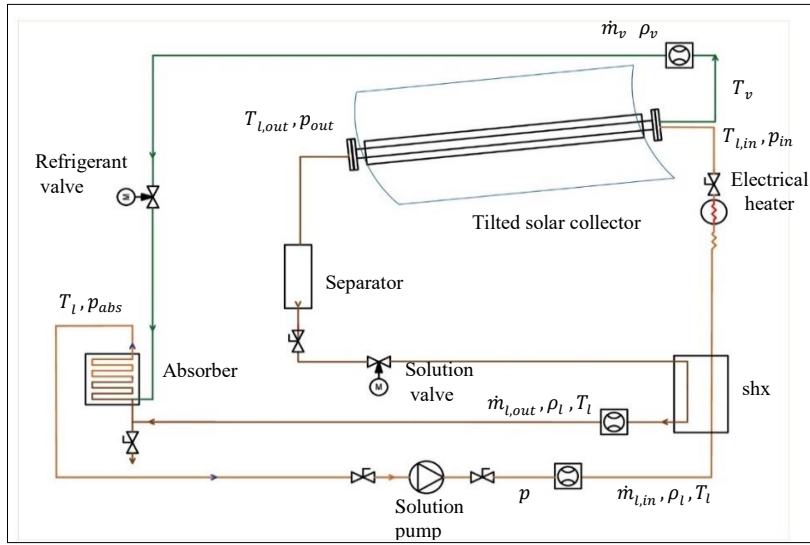


Fig. 6 Experimental setup

4. Results

A first set of data has been obtained during different days under a wide range of operating conditions. The solar generator operated with a mass flow rate \dot{m}_{lin} varying from 0.008 to 0.026 kg s⁻¹ at different pressures p_{in} , going from 10 to 20 bar. Inlet ammonia mass fraction slightly and smoothly oscillated around $x_{in} \sim 0.5$. The direct solar irradiance on the collector surface G_{bT} , with a tilt angle of 40°, varied from 480 to 900 W m⁻². Among the large set of data continuously recorded by the SCADA, only data referred to quasi-steady-state operation are considered for the present analysis. Representative operating points are obtained from selected data by a time-average over intervals of 2 minutes, in order to limit spurious effects. The ammonia vapor mass flow rate \dot{m}_v as well as the liquid solution temperature difference between tube inlet and outlet $\Delta T_l = T_{l,out} - T_{l,in}$, are considered as main outputs to characterize the solar generator performances. In order to present the results in a compact way, two parameters are defined to account for input conditions (Eq. 1). L_{sub} indicates the approximated length of the eventual subcooled region downstream the tube entrance. In fact, the liquid solution can enter the receiver tube under subcooled conditions $T_{l,in} < T_s(x_{in}, p)$ requiring to be heated up to the saturation temperature $T_s(x_{in}, p)$ before the evaporation begins. The effective collector length where ammonia generation takes place is then estimated as $L_t - L_{sub}$. A non-dimensional load parameter Λ is defined accounting for liquid solution mass flow rate over the solar power available.

$$L_{sub} = \frac{(T_s(x_{in}, p) - T_{l,in})\dot{m}_{l,in}c_{pl,s}}{G_{bT}L_a\eta_0} \quad \Lambda = \frac{\dot{m}_{l,in}c_{pl}(T_s, x_{in})T_s(x_{in}, p)}{G_{bT}L_a(L_t - L_{sub})}; \quad (\text{eq.1})$$

Fig. 7 shows the ammonia generation in terms of percentage of liquid solution mass flow rate evaporated $\dot{m}_{vR} = 100 \dot{m}_v / \dot{m}_{lin}$. Ammonia evaporation goes from 1.2% up to 5.6% of the inlet liquid solution mass flow rate. Higher evaporation rates are obtained for low load parameter values, corresponding to high solar irradiance and/or low liquid mass flow rate.

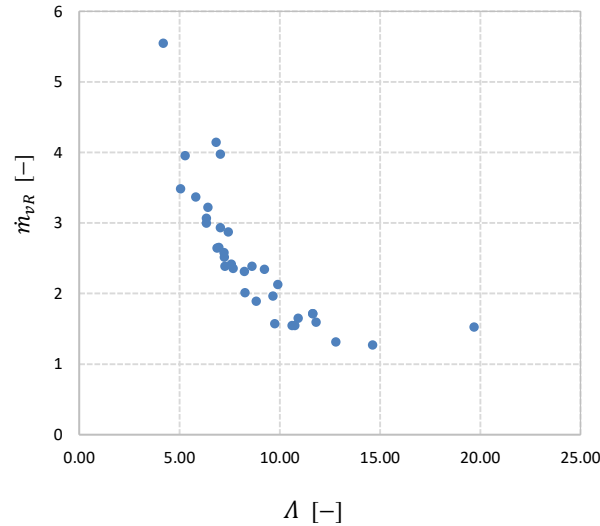


Fig. 7. Relative ammonia mass flow rate vs. load parameter.

Since ammonia mass fraction x in the liquid solution decreases downstream, as a result of evaporation, the saturation temperature increases accordingly for near-constant pressure conditions $T_s(x, p)$. As a consequence, a nonnegligible part of incoming thermal energy goes as sensible heat to the liquid solution, increasing its temperature under saturation conditions. ΔT_l decreases for higher Λ as more liquid solution is heated for a given solar power, as shown in Fig.8. The experimental results are coherent with the numerical simulation and the theoretical analysis previously developed and cited above.

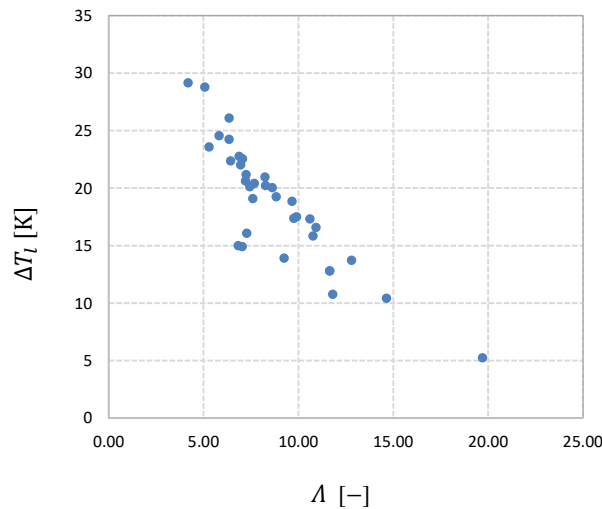


Fig. 8. Liquid dissolution temperature difference vs. load parameter.

5. Conclusions

The innovative concept of direct solar vapor generator proposed reduces the complexity and the cost of solar-driven absorption machines, eliminating the need of the heat transfer fluid as well as a heat exchanger, commonly need for this type of installations.

The presented layout has been applied to Ammonia/Lithium Nitrate working pair in order to benefit from the

promising performance of this type of AM. In this work, an experimental study of the proposal has been carried out using a simplified prototype approaching the working condition of a real air-cooled single effect AM.

The results demonstrate the practical feasibility of the proposed layout and encourage further investigation.

Ammonia evaporation rates going from 1% to 6% of the circulating solution mass flow rate have been obtained using a parabolic trough collector of holding 3 m length and 1.3 m aperture width under various irradiance conditions and tilting angles.

A downstream increase of liquid solution temperature has been measured and theoretically anticipated, which can be beneficial for preheating the incoming liquid flow to the generator when a recovery heat exchanger would be installed.

The results obtained and presented in this work have been useful for verifying and tuning the 1D numerical model developed. With their joint application, it is possible a full optimization of innovative direct refrigerant generators using solar collectors for absorption machines.

6. References

- National Renewable Energy Laboratories (NREL). (2015). *Parabolic Trough Collector Cost Update for the System Advisor Model (SAM)*. NREL. Golden, CO, USA: NREL. Retrieved from <https://www.nrel.gov/docs/fy16osti/65228.pdf>
- Best, R., & Rivera, W. (2015). A review of thermal cooling systems. *Applied Thermal Engineering*, 75, 1162-1175. doi:<http://dx.doi.org/10.1016/j.applthermaleng.2014.08.018>
- Dorra, H., Lee, S. C., & Bankoff, S. (1993). *A critical review of predictive models for the onset of significant void in forced-convection subcooled boiling*. doi:10.2172/10194563
- Famiglietti, A., Lecuona-Neumann, A., Nogueira, J. I., & Celik, S. B. (2018). Direct ammonia vapor generation inside a concentrating parabolic trough solar collector for an ammonia/lithium nitrate absorption machine. Theoretical study. Valencia.
- Herold, K. E., Radermacher, R., & Klein, S. A. (2016). *Absorption chillers and heat pumps*. CRC press.
- Hsu, Y. Y. (1962). On the size range of active nucleation cavities on a heating surface. *Journal of Heat Transfer*, 84(3), 207-213. doi:10.1115/1.3684339
- Lecuona, A., Famiglietti, A., & Legrand, M. (2019, May). Theoretical study of direct vapor generation for energy integrated solar absorption machines. *Renewable Energy*, 135, 1335-1353. doi:10.1016/j.renene.2018.09.056
- Libotean, S., Salavera, D., Valles, M., Esteve, X., & Coronas, A. (2007). Vapor-Liquid Equilibrium of Ammonia + Lithium Nitrate + Water and Ammonia + Lithium Nitrate Solutions from (293.15 to 353.15) K. *Journal of Chemical Engineering Data*, 52(3), 1050-1055. doi:10.1021/je7000045
- Mauthner, F., & Weiss, W. (2013). *Solar Heat Worldwide. Markets and Contribution to the Energy Supply 2011*. International Energy Agency. Paris: International Energy Agency. Solar Heating and Cooling Programm.
- Ventas, R., Lecuona, A., Vereda, C., & Rodriguez-Hidalgo, M. (2017). Performance analysis of an absorption double-effect cycle for power and cold generation using ammonia/lithium nitrate. *Applied Thermal Engineering*, in press. doi:<http://dx.doi.org/10.1016/j.applthermaleng.2016.12.102>
- Ventas, R., Vereda, C., Lecuona, A., & Venegas, M. (2011). Experimental study of a thermochemical compressor for an absorption/compression hybrid cycle. *Applied Energy*, 97, 297-304. doi:<https://doi.org/10.1016/j.apenergy.2011.11.052>

Wu, W., Wang, B., Shi, W., & Li, X. (2014). An overview of ammonia-based absorption chillers and heat pumps. *Renewable and Sustainable Energy Reviews*, 31(6), 81-707.